PUBLICATION OR PRESENTATION RELEASE REQUEST

Pubkey: 5959

NRLINST 5600.2

1. REFERENCES AND ENCLOSURES

Ref: (a) NRL Instruction 5600.2
(b) NRL Instruction 5510.40D

Encl: (1) Two copies of subject paper (or abstract)

2. TYPE OF PUBLICATION OR PRESENTATION

( ) Abstract only, published
( ) Book
( ) Conference Proceedings (refereed)
( ) Invited speaker
(X) Journal article (refereed)
( ) Oral Presentation, published
( ) Other, explain
( ) Abstract only, not published
( ) Book chapter
( ) Conference Proceedings (not refereed)
( ) Multimedia report
( ) Journal article (not refereed)
( ) Oral Presentation, not published

3. ADMINISTRATIVE INFORMATION

STRN NRL/JA/7330-08-9007
Route Sheet No. 7330/
Job Order No. 73-6867-07-5
Classification X U C
Sponsor ONR
approval obtained yes X no

4. AUTHOR

Title of Paper or Presentation
Characterizations of Minerogenic Particles in Support of Modeling Light Scattering in Lake Superior Through a Two-Component Approach

Author(s) Name(s) (*First,MI,Last*), Code, *Affiliation if not NRL*
Feng Peng, Steven Effler, David O'Donnell, Alan D. Weidemann, Martin Auer

It is intended to offer this paper to the ____________
(Name of Conference)

____
(Date, Place and Classification of Conference)

and/or for publication in **Limnology and Oceanography, Unclassified**
(Name and Classification of Publication) *(Name of Publisher)*

After presentation or publication, pertinent publication/presentation data will be entered in the publications data base, in accordance with reference (a).
It is the opinion of the author that the subject paper (is ____) (is not ___X) classified, in accordance with reference (b).
This paper does not violate any disclosure of trade secrets or suggestions of outside individuals or concerns which have been communicated to the Laboratory in confidence. This paper (does ____) (does not ___X) contain any militarily critical technology.
This subject paper (has ____) (has never _X_) been incorporated in an official NRL Report.

Alan D. Weidemann, 7333 Alan D. Weidemann
Name and Code *(Principal Author)* (Signature)

5. ROUTING/APPROVAL

CODE	SIGNATURE	DATE	COMMENTS
Author(s) Weidemann	Alan D. Weidemann	8 Oct 08	Need by 31 Oct 08 Publicly accessible sources used for this publication
Section Head			
Branch Head Teague, acting **Robert A Arnone, 7330**	William J Teague	10/8	
Division Head **Ruth H. Preller, 7300**		10/8/08	1. Release of this paper is approved. 2. To the best knowledge of this Division, the subject matter of this paper (has ____) (has never _X_) been classified.
Security, Code **1226**			1. Paper or abstract was released. 2. A copy is filed in this office. 550 403.8
Office of Counsel,Code **1008.3**	A Beede	10/16/08	
ADOR/Director NCST **E. R. Franchi, 7000**			
Public Affairs *(Unclassified/ Unlimited Only)*, Code **7030.4**			
Division, Code			
Author, Code			

HQ-NRL 5511/6 (Rev. 12-98) (e) THIS FORM CANCELS AND SUPERSEDES ALL PREVIOUS VERSIONS

08-1226-3351

PUBLICATION OR PRESENTATION RELEASE REQUEST

Pubkey: 5959

NRLINST 5600.2

1. REFERENCES AND ENCLOSURES	2. TYPE OF PUBLICATION OR PRESENTATION		3. ADMINISTRATIVE INFORMATION
Ref: (a) NRL Instruction 5600.2 (b) NRL Instruction 5510.40D Encl: (1) Two copies of subject paper (or abstract)	☐ Abstract only, published ☐ Book ☐ Conference Proceedings (refereed) ☐ Invited speaker ☒ Journal article (refereed) ☐ Oral Presentation, published ☐ Other, explain	☐ Abstract only, not published ☐ Book chapter ☐ Conference Proceedings (not refereed) ☐ Multimedia report ☐ Journal article (not refereed) ☐ Oral Presentation, not published	STRN NRL/JA/7330-08-9007 Route Sheet No. 7330/ Job Order No. 73-6867-07-5 Classification X U C Sponsor ONR Basic [illegible] approval obtained yes X no

4. AUTHOR

Title of Paper or Presentation

Characterizations of Minerogenic Particles In Support of Modeling Light Scattering In Lake Superior Through a Two- Component Approach

Author(s) Name(s) *(First,MI,Last), Code, Affiliation if not NRL*

Feng Peng, Steven Effler, David O'Donnell, Alan D. Weidemann, Martin Auer

This is a Final Security Review
Any changes made in the document
after approved by Code 1226
nullify the Security Review

It is intended to offer this paper to the ______ *(Name of Conference)*

______ *(Date, Place and Classification of Conference)*

and/or for publication in Limnology and Oceanography, Unclassified *(Name and Classification of Publication)* ______ *(Name of Publisher)*

After presentation or publication, pertinent publication/presentation data will be entered in the publications data base, in accordance with reference (a).

It is the opinion of the author that the subject paper (is ____) (is not __X_) classified, in accordance with reference (b).

This paper does not violate any disclosure of trade secrets or suggestions of outside individuals or concerns which have been communicated to the Laboratory in confidence. This paper (does ____) (does not __X_) contain any militarily critical technology.

This subject paper (has ____) (has never _X_) been incorporated in an official NRL Report.

Alan D. Weidemann, 7333 — Name and Code *(Principal Author)*

Alan D. Weidemann (Signature)

5. ROUTING/APPROVAL

CODE	SIGNATURE	DATE	COMMENTS
Author(s) Weidemann	Alan D. Weidemann	8 Oct 08	Need by 31 Oct 08 Publicly accessible sources used for this publication
			Personally identifying email addresses may not be posted to publicly accessible DON websites per SECNAVINST 5720.47B, encl. (1); 3.d.(7)
Section Head			
Branch Head Teague, acting Robert A Arnone, 7330	William J Teague	10/8	
Division Head Ruth H. Preller, 7300	(Acting)	10/8/08	1. Release of this paper is approved. 2. To the best knowledge of this Division, the subject matter of this paper (has ____) (has never _X_) been classified.
Security, Code 1226		10/14/08	1. Paper or abstract was released. 2. A copy is filed in this office.
Office of Counsel, Code 1008.3	A Beede	10/16/08	
ADOR/Director NCST E. R. Franchi, 7000			
Public Affairs *(Unclassified/ Unlimited Only)*, Code 7030.4		10/21/08	add NRL & Ett to acknowledgment
Division, Code			
Author, Code			

HQ-NRL 5511/6 (Rev. 12-98) (e)

THIS FORM CANCELS AND SUPERSEDES ALL PREVIOUS VERSIONS

S

REPORT DOCUMENTATION PAGE	*Form Approved* *OMB No. 0704-0188*

1. REPORT DATE *(DD-MM-YYYY)* 13-08-2009	**2. REPORT TYPE** Journal Article	**3. DATES COVERED** *(From - To)*

4. TITLE AND SUBTITLE Characterizations of Minerogenic Particles in Support of Modeling Light Scattering in Lake Superior Through a Two-Component Approach	**5a. CONTRACT NUMBER**
	5b. GRANT NUMBER
	5c. PROGRAM ELEMENT NUMBER 0602435N
6. AUTHOR(S) Feng Peng, Steven Effler, David O'Donnell, Alan D. Weidemann, Martin Auer	**5d. PROJECT NUMBER**
	5e. TASK NUMBER
	5f. WORK UNIT NUMBER 73-6867-07-5

7. PERFORMING ORGANIZATION NAME(S) AND ADDRESS(ES) Naval Research Laboratory Oceanography Division Stennis Space Center, MS 39529-5004	**8. PERFORMING ORGANIZATION REPORT NUMBER** NRL/JA/7330-08-9007
9. SPONSORING/MONITORING AGENCY NAME(S) AND ADDRESS(ES) Office of Naval Research 800 N. Quincy St. Arlington, VA 22217-5660	**10. SPONSOR/MONITOR'S ACRONYM(S)** ONR
	11. SPONSOR/MONITOR'S REPORT NUMBER(S)

12. DISTRIBUTION/AVAILABILITY STATEMENT

Approved for public release, distribution is unlimited.

20090821529

13. SUPPLEMENTARY NOTES

14. ABSTRACT

The role of suspended minerogenic particles in light scattering in eastern Lake Superior and Keweenaw Bay (11 sites) during July of 2006 was evaluated with an individual particle analysis technique (scanning electron microscopy interfaced with automated image and X-ray analyses, SAX), along with bulk measurements of particulate scattering and backscattering coefficients (bp and bbp) and chlorophyll a concentration ([Chl]). SAX measurements provided information on light-scattering attributes of minerogenic particles, including chemical composition and particle size distribution (PSD). The data were used in Mie theory calculations for estimations of minerogenic scattering and backscattering coefficients (bm and bb,m). The bay had higher concentrations of minerogenic particles and higher values of bm, bb,m, bbp, and the backscattering ratio (bbp : bp) than the pelagic sites. Minerogenic scattering was primarily attributable to clay mineral particles in the size range of 1 -10 mm. The PSDs deviated from the (Junge) pattern of monotonic increase of particle numbers with decreasing particle size. The estimates of bm and bb,m combined with those of organic particulate components, as represented by empirical Case 1 bio-optical models, showed reasonably good closure with bp and bbp, supporting the credibility of the SAX -Mie approach. Variations in the bbp : bp ratio are strongly related to spatial differences in the relative contributions of phytoplankton vs. minerogenic particles to scattering, with higher values observed where the minerogenic component is more important. SAX can advance the understanding of optical variability by establishing the contributions of well-defined minerogenic constituents that strongly influence optical properties.

15. SUBJECT TERMS

PSD, backscattering, inherent optical properties

16. SECURITY CLASSIFICATION OF:			**17. LIMITATION OF ABSTRACT**	**18. NUMBER OF PAGES**	**19a. NAME OF RESPONSIBLE PERSON**
a. REPORT	**b. ABSTRACT**	**c. THIS PAGE**			Alan D. Weidemann
Unclassified	Unclassified	Unclassified	UL	13	**19b. TELEPHONE NUMBER** *(Include area code)* 228-688-6232

Limnol. Oceanogr., 54(4), 2009, 1369–1381

Characterizations of minerogenic particles in support of modeling light scattering in Lake Superior through a two-component approach

Feng Peng,[a,*] Steve W. Effler,[a] David O'Donnell,[a] Alan D. Weidemann,[b] and Martin T. Auer[c]

[a] Upstate Freshwater Institute, Syracuse, New York
[b] Naval Research Laboratory, Stennis Space Center, Mississippi
[c] Department of Civil and Environmental Engineering, Michigan Technological University, Houghton, Michigan

Abstract

The role of suspended minerogenic particles in light scattering in eastern Lake Superior and Keweenaw Bay (11 sites) during July of 2006 was evaluated with an individual particle analysis technique (scanning electron microscopy interfaced with automated image and X-ray analyses, SAX), along with bulk measurements of particulate scattering and backscattering coefficients (b_p and b_{bp}) and chlorophyll *a* concentration ([Chl]). SAX measurements provided information on light-scattering attributes of minerogenic particles, including chemical composition and particle size distribution (PSD). The data were used in Mie theory calculations for estimations of minerogenic scattering and backscattering coefficients (b_m and $b_{b,m}$). The bay had higher concentrations of minerogenic particles and higher values of b_m, $b_{b,m}$, b_{bp}, and the backscattering ratio ($b_{bp}:b_p$) than the pelagic sites. Minerogenic scattering was primarily attributable to clay mineral particles in the size range of 1–10 μm. The PSDs deviated from the (Junge) pattern of monotonic increase of particle numbers with decreasing particle size. The estimates of b_m and $b_{b,m}$ combined with those of organic particulate components, as represented by empirical Case 1 bio-optical models, showed reasonably good closure with b_p and b_{bp}, supporting the credibility of the SAX–Mie approach. Variations in the $b_{bp}:b_p$ ratio are strongly related to spatial differences in the relative contributions of phytoplankton vs. minerogenic particles to scattering, with higher values observed where the minerogenic component is more important. SAX can advance the understanding of optical variability by establishing the contributions of well-defined minerogenic constituents that strongly influence optical properties.

Light scattering by particles is a fundamental feature of radiative transfer in water and the attendant signal available for remote sensing. Two important metrics of light scattering are the total particulate scattering and backscattering coefficients (b_p and b_{bp}; m^{-1}) that represent integrations over the angular range of $0-\pi$ and $\pi/2-\pi$, respectively, of the volume-scattering function (VSF, β). The backscattering ratio, $b_{bp}:b_p$ ($\tilde{b}_{bp}$), has recently been used as a diagnostic to infer particle composition (Boss et al. 2004; Loisel et al. 2007; Whitmire et al. 2007), model the underwater light field (Mobley et al. 2002), and explain remote-sensing variability in coastal areas (Lubac and Loisel 2007). These optical properties depend on various attributes of the particle population, including the composition, particle size distribution (PSD), particle shape and inhomogeneity, and number concentration (N), with the exception that $\tilde{b}_{bp}$ is independent of N.

Aquatic ecosystems represent complex media with respect to particulate scattering because of the great heterogeneity of particle characteristics that influence related optical properties differently (Stramski et al. 2004*a*, 2007; Peng and Effler 2007). The extent to which differences in bulk optical properties can be explained by bulk properties of a particle population such as concentrations of chlorophyll *a* ([Chl]) or suspended particulate matter is limited (Babin et al. 2003; Stramski et al. 2007). Moreover, such metrics provide little insight into the roles of the various particle types in regulating these optical properties.

Stramski et al. (2001, 2004*a*, 2007) have advocated a reductionist approach of increased partitioning of inherent optical properties (IOPs) into a 'certain manageable number' of important functional constituents. Though the partitioning of b_p (or b_{bp}) into organic and minerogenic scattering coefficients (b_o and b_m)

$$b_p = b_o + b_m \tag{1}$$

is more rudimentary than the goals of the reductionist approach, such an effort has rarely been rigorously applied to real systems (Peng et al. 2007; Snyder et al. 2008; Stavn and Richter 2008). A reductionist version of Eq. 1 would further partition organic and minerogenic particulate components into more constituents. Stramski et al. (2001) implemented the reductionist approach in a modeling analysis of IOPs, focusing primarily on partitioning of planktonic contributions while including the effects of minerogenic particles through reasonable assumptions of their characteristics. These model simulations yielded insights on optical variability of the ocean and suggested that minerogenic particles were potentially important in regulating b_{bp}, occasionally even in open ocean waters. Subsequently, these investigators have further evaluated the potential origins, optical properties, and implications for remote sensing of terrigenous minerogenic particles in seawater (Stramski et al. 2004*b*, 2007; Woźniak and Stramski 2004). In a field study to understand the observed IOP variability in New England continental shelf waters, Green et al. (2003) conducted direct individual particle analyses and included a mineral group in their five particles

---

[*] Corresponding author: fpeng@upstatefreshwater.org

types. Their findings emphasized the necessity to measure mineral particles for full understanding of backscattering variations in the ocean.

Minerogenic particles play even greater (sometimes dominant) roles in regulating light scattering in coastal Case 2 (Stramski et al. 2001; Loisel et al. 2007) and inland waters (Kirk 1994; Peng and Effler 2005; Peng et al. 2007). In even the most dilute and highest clarity lacustrine systems, minerogenic particles strongly influence apparent optical properties (AOPs; Swift et al. 2006), including remote-sensing signals (Li et al. 2004). Bukata et al. (1978) recognized the importance of suspended minerals in shaping the underwater and above-water light fields of Lake Superior, and included an inorganic particulate component in the development of a semi-empirical model. Recently, an individual particle analysis (IPA) technique, scanning electron microscopy interfaced with automated image and X-ray analyses (SAX), has been used to directly measure the light-scattering attributes (N, PSD, composition, and shape) of minerogenic particles of sizes >0.2 μm in several inland waters (Peng and Effler 2007; Peng et al. 2007). SAX results served as inputs to Mie-theory calculations of the scattering and backscattering efficiency factors (Q_{bm} and Q_{bbm}, dimensionless) of individual particles, supporting direct estimates of spectral b_{m} and the minerogenic backscattering coefficient ($b_{\mathrm{b,m}}$), as described for b_{m} below

$$b_{\mathrm{m}}(\lambda)=\frac{1}{V}\sum_{i=1}^{N_{\mathrm{m}}} Q_{\mathrm{bm},i}(m_i,\lambda,d_i)\mathrm{PA}_{\mathrm{m},i} \qquad (2)$$

where λ is the wavelength of light, N_{m} is the number of minerogenic particles per unit volume of water (number m^{-3}), $\mathrm{PA}_{\mathrm{m},i}$ is the projected area of minerogenic particle i, and V is the sample volume. Likewise, $b_{\mathrm{b,m}}(\lambda)$ was calculated with the backscattering efficiency factor, $Q_{\mathrm{bbm},i}$. These two efficiency factors of a particle depend on its size (d) and (relative) complex refractive index (m, depends on the composition of the particle), and on λ. Moreover, SAX supports partitioning of b_{m} and $b_{\mathrm{b,m}}$ into multiple minerogenic particles types, such as clay minerals, quartz, and calcite (Peng et al. 2007), consistent with the goals of the reductionist approach. The integrated SAX–Mie method has been described as precursor work for advancing the reductionist approach (Stramski et al. 2007).

Establishment of the representativeness of the SAX–Mie estimates of b_{m} and $b_{\mathrm{b,m}}$ is central to advancing the implementation of the reductionist approach. Some progress has been reported recently in this regard for a limited number of particle-rich inland waters (Peng and Effler 2007; Peng et al. 2007). Demonstrations for most natural systems are complicated by noteworthy contributions of organic particles that are presently not readily amenable to the same level of independent individual particle characterizations. This issue was largely avoided in the study of one reservoir (Peng and Effler 2007) where minerogenic particles dominate, and reasonably good consistency between SAX–Mie estimates of b_{m} and bulk measurements of the attenuation coefficient at 660 nm, $c(660)$ (a reliable surrogate of b; Babin et al. 2003) was reported. In addition, summations of SAX–Mie-based estimates of $b_{\mathrm{m}}(650)$ and organic particulate scattering, as estimated by an empirical bio-optical [Chl]-based model developed for Case 1 waters (Loisel and Morel 1998), showed good closure with bulk measurements of $b_{\mathrm{p}}(650)$ for several inland waters enriched in particles (Peng et al. 2007). Similar closure efforts have to date not been attempted in evaluating the representativeness of SAX–Mie estimates of $b_{\mathrm{b,m}}(\lambda)$. Success in such closure efforts would result in a simple two-component model that could estimate b_{p} and b_{bp} and resolve contributions of minerogenic and organic particles based on SAX and [Chl] measurements.

This paper documents the light-scattering features of minerogenic particles assessed by SAX, and bulk measurements of b_{p}, b_{bp}, and [Chl], for pelagic near-surface waters of oligotrophic Lake Superior and one of its major embayments. The SAX–Mie-based estimates of b_{m} and $b_{\mathrm{b,m}}$ are tested for consistency through the use of Case 1 empirical bio-optical models to independently estimate b_{o} and the organic backscattering coefficient ($b_{\mathrm{b,o}}$) from [Chl] and by comparing the summations of the minerogenic and organic components with bulk measurements of b_{p} and b_{bp}. Contributions to b_{m} and $b_{\mathrm{b,m}}$ from particle classes that are based on composition and size are resolved, and the dependence of spatial differences of $\tilde{b}_{\mathrm{bp}}$ on metrics of composition of the particulate assemblage is evaluated. Lastly, the role of minerogenic particles in influencing light-scattering levels in Lake Superior and related implications for remote sensing are considered. This paper advances earlier SAX-based light-scattering studies (Peng and Effler 2007; Peng et al. 2007) by extending to more dilute conditions, addressing closure for estimates of b_{bp} and demonstrating the interplay between minerogenic particle contributions and $\tilde{b}_{\mathrm{bp}}$.

Methods

Study system, sampling, and field measurements—Lake Superior is the westernmost (48°00′N, 88°00′W), largest, and most oligotrophic of the Laurentian Great Lakes. Its residence time is ~200 yr. Water clarity is relatively high (Secchi depth 15–20 m) in pelagic areas of the lake. The role of the minerogenic particle population in light scattering in the lake has not been characterized. Lake Superior has been described as optically complex (Case 2; Li et al. 2004). In particular, absorption by chromophoric dissolved organic matter (CDOM) is high relative to that associated with phytoplankton pigments (Gons et al. 2008) and sediment is believed to contribute to local remote-sensing signatures (Budd 2004), though lake wide effects are uncertain (Li et al. 2004).

A total of 11 sites (Fig. 1) were visited over the interval of 05–14 July in 2006. These included two locations in the Keweenaw Waterway (KW) proximate to a major tributary inflow (the Sturgeon River; Fig. 1), six sites along the axis of Keweenaw Bay (KB), and three pelagic sites in eastern Lake Superior (ELS). Site KW1 reflects the local effects of the Sturgeon River inflow to Keweenaw Bay through the Keweenaw Waterway. Site KW2 is a proximate (within 1 km) nearshore bay location, included to provide contrast

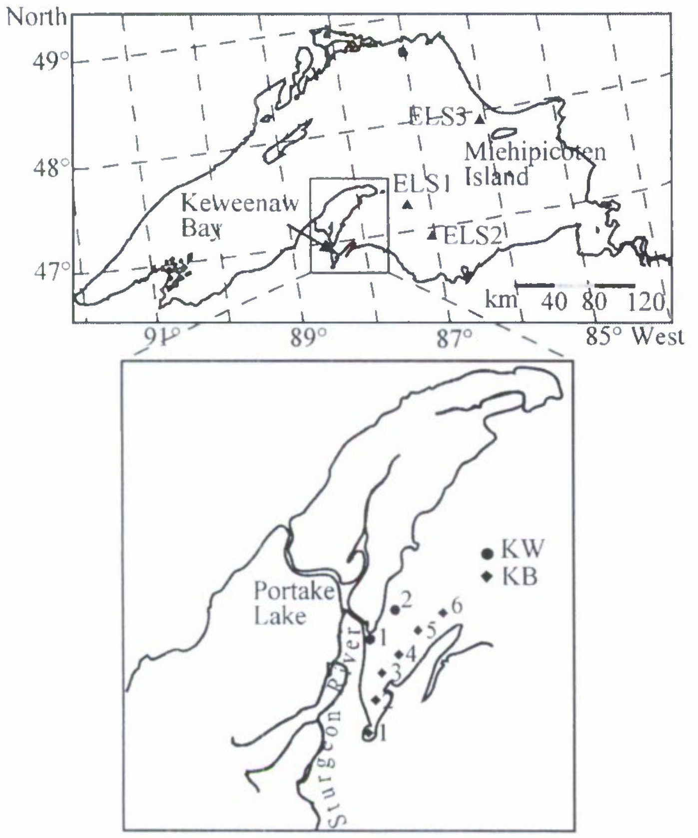

Fig. 1. Map of Lake Superior with sampling sites in Keweenaw Waterway (KW; two sites), Keweenaw Bay (KB; six sites), and Eastern Lake Superior (ELS; three sites).

to KW1. The other bay sites extended along a transect from the inner-(KB1) to outer-bay (KB6) bounds (~33 km). The three pelagic sites in eastern Lake Superior (ELS; shelf and profundal locations) extend over ~155 km from Michipicoten Island (Fig. 1). At each site in situ optical measurements were conducted and near-surface samples were collected for IPA and [Chl] (Parsons et al. 1984) analyses.

Spectral attenuation, absorption, and backscattering coefficients [$c(\lambda)$, $a(\lambda)$, and $b_b(\lambda)$; m^{-1}] were measured with a combined instrument package (single profiling cage, integrated outputs) consisting of an ac-s (spectral absorption and attenuation meter) and a BB9 (backscattering meter) from WET Labs. Backscattering measurements were unavailable for the two KW sites. The ac-s measures $c(\lambda)$ and $a(\lambda)$ (25-cm path length) relative to pure water, with a spectral resolution of 4 nm over the range of 400–730 nm. This instrument was calibrated according to guidelines of the manufacturer with pure water and checked between deployments following the manufacturer's calibration protocol (WET Labs, Inc. 2006). Adjustments for the effects of temperature on pure water absorption and attenuation were made according to Pegau et al. (1997). The absorption spectra were corrected for scattering error following the manufacturer's protocols. The spectral particulate scattering coefficient, $b_p(\lambda)$, was determined by difference, $c(\lambda) - a(\lambda)$. The BB9 measured VSF at 117° [$\beta_p(117°, \lambda)$] at nine discrete wavelengths, for which $c(\lambda)$ and $a(\lambda)$ measurements were made. The angle of 117° has been identified as a minimum convergence point for variations in $\beta(\theta, \lambda)$ caused by suspended particles. Backscattering [$b_{bp}(\lambda)$] was calculated from $\beta_p(117°, \lambda)$ according to $b_{bp}(\lambda) = 2\pi\chi\beta_p(117°,\lambda)$, where $\chi = 1.1$ (Boss and Pegau 2001). Corrections for attenuation along the path from the light source to the sample volume and then to the detector were made based on $a(\lambda)$ measurements from the ac-s (WET Labs, Inc. 2007). Values of b_p and b_{bp} reported here are averages of those collected over a 0.5-m depth interval in near-surface waters.

SAX protocols—Sample preparation and instrumentation methodology for SAX have been described previously (Peng and Effler 2005, 2007), and are only briefly reviewed here. Suspended particles from known volumes of water samples were deposited onto polycarbonate membranes (0.4-μm pore size) by pressure filtration, air-dried, and coated with carbon. The SAX instrumentation was an Aspex PSEM 2000 system controlled by automated feature analysis (AFA) software (Aspex®). About 2000 individual particles were analyzed for each of the 10 samples (no water sample from KW2 was available) for both morphology and composition characteristics (~3 h per sample).

Based on a rotating chord algorithm, AFA represents each particle by a series of radiating triangles formed by the particle's centroid and 16 chords drawn through the centroid to the edges of the particle at 11° increments. The projected area (PA$_i$; m^2) of a particle is measured as the sum of all triangular areas. Particle size (d_i; μm) is defined as the circular area equivalent diameter. Particle shape is described here by the aspect ratio (ASP), the ratio of the length of the longest chord to that of its orthogonal chord. The ASP value is a measure of a particle's deviation from sphericity (ASP of a sphere is 1).

Composition of individual minerogenic particles is assessed by SAX from acquisition of X-ray counts of 16 elements (Na and higher atomic numbers, including Al, Si, Ca, Fe, Mn), and is represented by its normalized elemental X-ray counts. Based on their elemental X-ray composition, minerogenic particles were sorted into five predefined generic minerogenic particle types (Peng et al. 2007), with assigned values of m ($m = n - n'i$, where n and n' are the real and imaginary parts of m): 'Clay' (aluminum silicates, $m = 1.173 - 0.001i$); 'Quartz' (mineral SiO_2, $m = 1.155 - 0.0001i$); 'Si-rich' (Si-containing minerals, assumed $m = 1.173 - 0.001i$); 'Ca-rich' (particles contain ≥40% Ca X-rays, $m = 1.19 - 0.0005i$); and 'Misc' (miscellaneous inorganic particles, assumed $m = 1.173 - 0.001i$). Specification of m values for these particle types was based on literature compilations (Kerr and Rogers 1977; Woźniak and Stramski 2004). 'Diatom' particles were differentiated from 'Quartz' (both have >90% Si X-rays) based on their lower X-ray densities (Peng et al. 2002). Hereafter particles in the 'Clay' class are described as clay mineral particles (e.g., kaolinite), a chemical grouping that differs from the use of 'clay' to describe a particle size group.

A useful bulk property of an analyzed sample is the total particle projected area concentration, or the particle projected area per unit volume of water (PAV; m^{-1}), a metric that is approximately proportional to the magnitude of light attenuation (Peng and Effler 2007) and remote-sensing reflectance (Sydor and Arnone 1997). SAX measurements support determination of the PAV associated with each of the specified minerogenic particle types. The minerogenic component of PAV (PAV_m) is the summation of values for the five specified particle types.

PSDs and scattering calculations—PSDs of minerogenic particles are presented as a size distribution function (or density function), $F(d) = 1/V \times \Delta N/\Delta d$, where N is the total number of minerogenic particles in V, and ΔN is the number of mineral particles in a size interval of Δd. Size distributions were extended to particles >0.2 μm, a size somewhat smaller than the nominal pore size of the used filters. Atteia et al. (1998) demonstrated that particles much smaller than the respective pore sizes of the membrane filters were retained. In paired measurements of samples collected on 0.2-μm- and 0.4-μm-pore–sized filters, we have found that particles in the 0.2–0.4-μm size range were only slightly underrepresented by the 0.4-μm-pore–sized filter, and that the general PSD patterns were not affected by the filter pore size. Results presented here for the 0.2–0.4-μm size interval are not presented as quantitative but serve to depict the general pattern for these small particles.

The minerogenic particle-scattering and backscattering coefficients (b_m and $b_{b,m}$) were calculated from SAX results according to Eq. 2. Values of the efficiency factors $Q_{bm,i}$ and $Q_{bbm,i}$ were obtained from the BHMie algorithm by Bohren and Huffman (1983), based on Mie theory for homogenous spheres. Scattering calculations and field observations are reported here for $\lambda = 650$ nm; reference to wavelength is omitted hereafter.

Adjustments of PA_i values were made to accommodate the effect of the preferred orientation (lying flat) of mineral particles on the filter membranes (Jonasz 1987), based on the ASP values of the particle: if ASP ≥ 1.5, then $PA_i^* = 0.8 \times PA_i$, where PA_i^* is the adjusted PA value for the ith particle (Peng et al. 2007). Average scattering efficiency factors of the minerogenic particle populations ($<Q_{b,m}>$ and $<Q_{bb,m}>$) of each site were calculated as the ratios of b_m and $b_{b,m}$ to PAV_m. These average efficiency values reflect the combined effects of PSD and chemical composition.

Empirical bio-optical models for scattering (Loisel and Morel 1998) and backscattering (Morel and Maritorena 2001) coefficients as functions of [Chl] for Case 1 (open ocean) waters were applied here as estimators of the organic components of b_p and b_{bp} (i.e., b_o and $b_{b,o}$).

$$b_o(650) = 0.347[\mathrm{Chl}]^{0.766}(660/650)0.97 \tag{3}$$

$$b_{b,o}(650) = \{0.002 + 0.01[0.50 - 0.25\log_{10}[\mathrm{Chl}]](650/550)^{v}\} \times b_o(550) \tag{4}$$

where

$$v = \begin{cases} 0.5(\log_{10}[\mathrm{Chl}] - 0.3) & \text{for } 0.02 \leq [\mathrm{Chl}] \leq 2 \text{ mg m}^{-3} \\ 0 & \text{otherwise} \end{cases} \tag{4a}$$

and

$$b_o(550) = 0.416[\mathrm{Chl}]^{0.766} \tag{4b}$$

The 0.97 adjustment in Eq. 3 accommodates the effect of replacing c in the original model with b. The summations of minerogenic and organic scattering and backscattering components were compared to bulk measurements of b_p (Eq. 1) and b_{bp} to evaluate the consistency of this forward modeling approach and the extent of closure.

Results

Light-scattering attributes of minerogenic particles—Light-scattering features of minerogenic particles collected from Lake Superior, as characterized by the SAX–Mie approach, are presented in Table 1. The composition of minerogenic particles is represented in the context of light-scattering implications by the relative contribution of the five particle types to PAV_m. The 'Misc' type contributed <12% to PAV_m, indicating that the adopted classification scheme performed well in categorizing the minerogenic particles in the lake. Generally uniform composition was observed (Table 1). Clay minerals ('Clay' class) dominated PAV_m for all the sites, representing an average of 73% (coefficient of variation, CV = 12%) of the total. The next largest contributors to PAV_m were the 'Quartz' and 'Si-rich' classes with the exception of site ELS3, where 'Ca-rich' was the second largest component.

Nonspherical morphology prevailed for the minerogenic particle populations of all the sites, as depicted by the mean ASP values (Table 1). Though the shapes of the minerogenic particles were diverse (Fig. 2A), as indicated by the relatively large standard deviation (SD) values, the mean ASP values were within a narrow range of 1.93–2.30, suggesting a similarity in the distribution of shapes. However, these deviations from sphericity of the minerogenic particles were modest relative to those observed for diatoms, whose large mean ASP values (several times greater than those for the minerogenic particle populations; Table 1) were attributed mostly to pennate forms (e.g., Fig. 2B).

Representative minerogenic PSDs are presented for a bay (KB6) and an open lake site (ELS3; Fig. 3). Monotonic increases in number density with the decrease in particle sizes, a pattern commonly described by the Junge function, were not observed. Instead, the PSDs exhibited right-skewed patterns. Peak densities were between 0.4 μm and 0.6 μm, around which greater and longer tailed decline in particle numbers for particles larger than the modal sizes prevailed. If the Junge function was fitted for particles larger than the peak density size, the slope values ($\sim$3) were consistent with those reported in the literature (Stramski and Kiefer 1991). Differences among sites were observed in number concentrations rather than the general shapes of PSDs (Fig. 3). Moreover, similar patterns prevailed for the various particle groups, as illustrated for the clay minerals at site KB6.

Calculated size dependencies of b_m (Fig. 4A) and $b_{b,m}$ (Fig. 4B) are presented for the same two samples in the

Table 1. Composition, morphology, size distribution, and scattering characteristics of suspended particle populations in Lake Superior (no observations for site KB2).

Site	PAV_m* (m^{-1})	PAV_m type distribution (%)					mean ASP±SD†		$<Q_{b,m}>$	$<Q_{bb,m}>$	$d_{50,bm}$ (μm)	$d_{50,bbm}$ (μm)
		Clay	Quartz	Si-rich	Ca-rich	Misc	Mineral	Diatom				
KW1	0.182	75.3	7.1	4.7	1.1	11.9	1.93±1.32	7.63±14.5	2.23	0.044	3.63	4.17
KW2	0.031	76.9	3.1	15.3	1.0	3.7	2.04±2.10	8.76±9.87	2.16	0.040	2.08	3.11
KB1	0.067	74.5	10.5	7.0	0.6	7.3	1.99±1.53	4.97±7.57	2.31	0.045	2.23	3.18
KB3	0.080	75.0	3.2	18.3	0.0	3.6	2.30±2.01	11.56±13.8	2.24	0.051	2.95	3.77
KB4	0.030	73.3	11.0	7.5	1.2	7.0	1.94±1.44	10.28±17.7	2.31	0.047	2.31	3.28
KB5	0.043	82.1	3.0	10.8	0.1	4.1	2.27±2.62	10.25±11.8	2.11	0.038	2.24	3.65
KB6	0.050	69.6	15.4	11.1	0.0	3.8	1.93±1.42	13.12±18.6	2.38	0.045	2.05	2.93
ELS1	0.016	64.3	5.8	13.0	5.7	11.2	1.94±2.42	9.45±15.0	2.36	0.050	2.39	3.39
ELS2	0.026	73.3	9.1	8.9	3.4	5.3	2.00±1.51	7.72±12.8	2.21	0.043	2.26	3.33
ELS3	0.022	54.7	6.3	14.8	17.7	6.5	2.12±2.29	10.58±12.0	2.38	0.047	2.19	3.13

* PAV_m: total projected area of minerogenic particles per unit volume of water.

† ASP: aspect ratio; SD: standard deviation.

format of cumulative contributions of particle size classes to scattering. Submicron particles and those larger than 10 μm made only minor (<10%) contributions to both b_m and $b_{b,m}$. The sizes that correspond to the 50th percentile of b_m (or median size of scattering, $d_{50,bm}$; Fig. 4A) and $b_{b,m}$ ($d_{50,bbm}$; Fig. 4B) are useful metrics in the evaluation of the relative importance of various particle sizes to scattering. These values were the highest in the inflow zone of the tributary, site KW1 (Table 1). Little variation was observed for the other sites, with the values of $d_{50,bbm}$ shifted ~1 μm larger than those of $d_{50,bm}$ (Table 1); the average values were 3.39 μm and 2.43 μm, respectively. No systematic spatial structure in these metrics was observed.

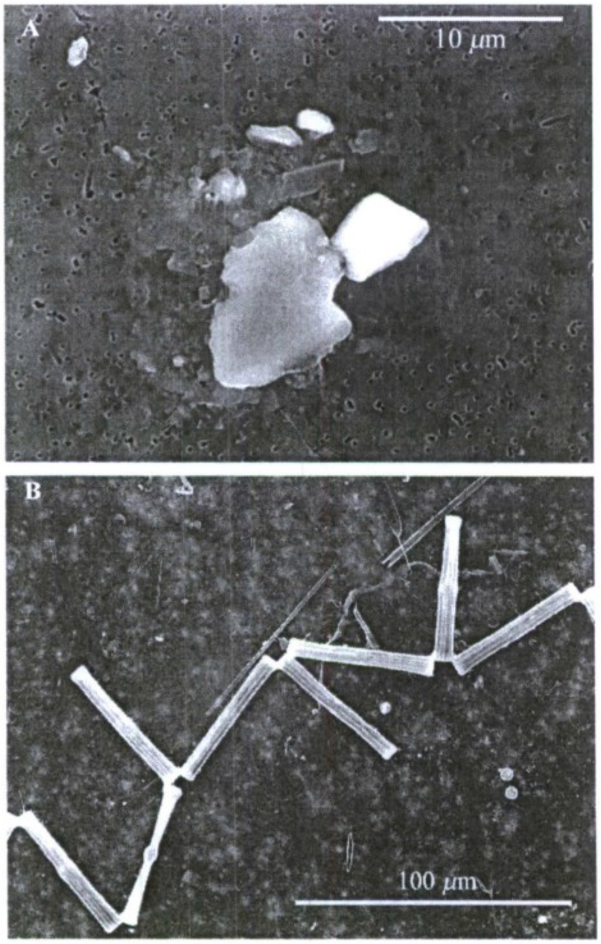

Fig. 2. Micrographs of selected particles by scanning electron microscopy: (A) inorganic particles, including a plate-like clay mineral, and (B) pennate diatoms (with high ASP values). Particles in (A) and (B) were from the sample collected from KW2 on 05 July 2006.

Spatial patterns of PAV_m, b_m, $b_{b,m}$, and bulk measures of scattering—Measurements of PAV_m (Fig. 5A) and coupled estimates of b_m (Fig. 5B) and $b_{b,m}$ (Fig. 5C) were the highest in the tributary inflow zone (site KW1) and the lowest in the open waters of eastern Lake Superior (ELS sites). The mean PAV_m for the five Keweenaw Bay (KB) sites was >two-fold greater than for the three ELS sites. There were substantial spatial differences in minerogenic particle levels and scattering within both the bay and eastern Lake Superior. The influence of the monitored tributary input (KW1; Fig. 1) on spatial structure in the bay at the time of sampling was small (Fig. 5A). The spatial

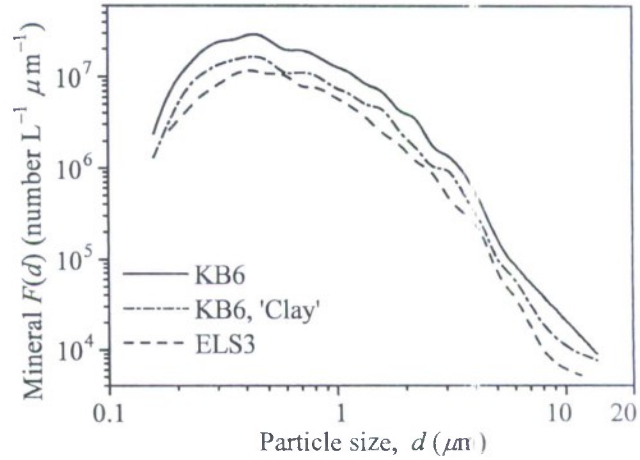

Fig. 3. Examples of mineral PSDs expressed in density function. Samples were from KB6 and ELS3 sites, and PSD of clay minerals ('Clay' class) from KB6 is also shown.

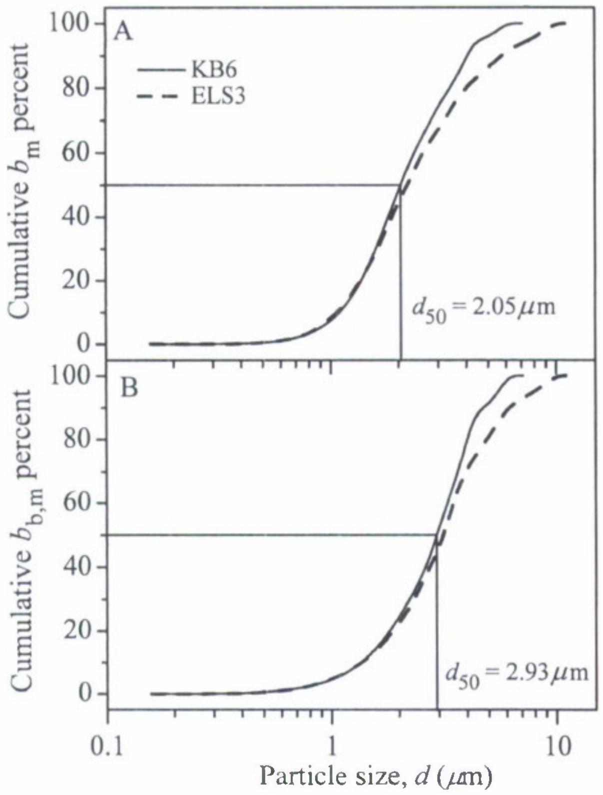

Fig. 4. Size dependency patterns of scattering for two sites, KB6 and ELS3: (A) cumulative b_m, and (B) cumulative $b_{b,m}$. The sizes that correspond to the 50th percentile of b_m and $b_{b,m}$ ($d_{50,bm}$ and $d_{50,bbm}$, respectively) are illustrated.

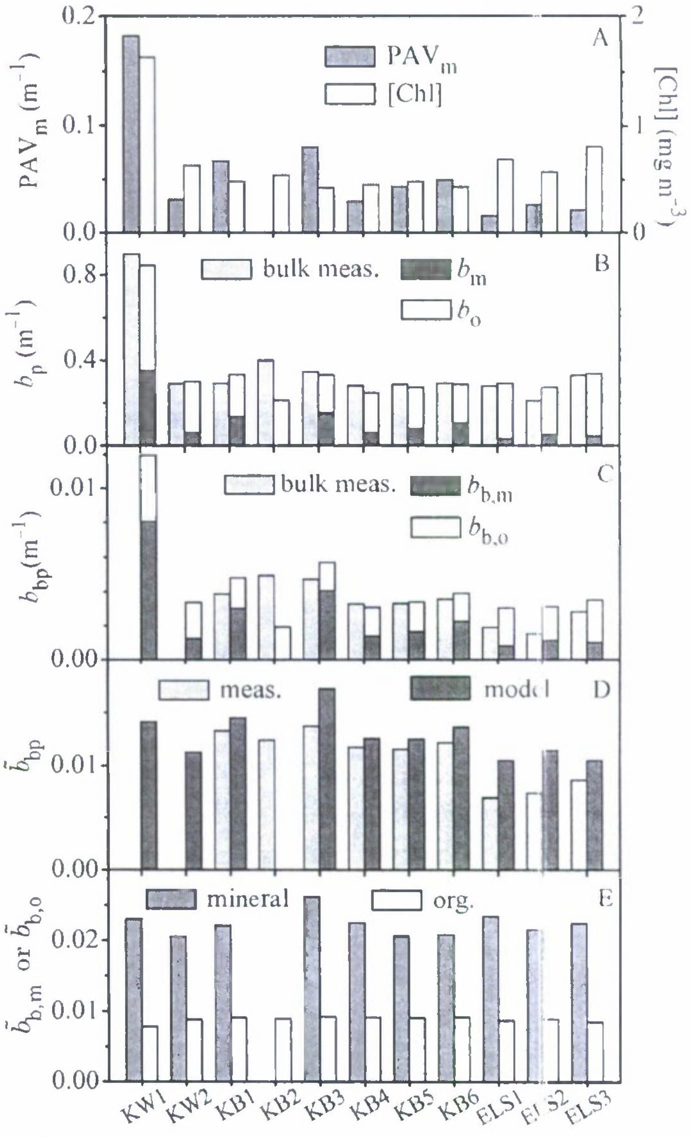

Fig. 5. Results of laboratory analyses, in situ optical measurements, and light-scattering modeling for study sites in Lake Superior: (A) PAV$_m$ and [Chl], (B) measured and modeled b_p, (C) measured and modeled b_{bp}, (D) backscattering ratio, from measurements and $(b_{b,o} + b_{b,m}) : (b_o + b_m)$, and (E) backscattering ratios of organic and minerogenic components.

patterns in the calculated values of b_m and $b_{b,m}$ (Fig. 5B,C) tracked linearly those observed for PAV$_m$ (Fig. 5A). Accordingly, the values of $<Q_{b,m}>$ and $<Q_{bb,m}>$ were uniform; the average values were 2.23 and 0.045, respectively, with CV values of 4.2% and 9.0%. Levels of [Chl] were somewhat higher at the ELS sites than in the bay (Fig. 5A); average concentrations were 0.69 mg m^{-3} and 0.63 mg m^{-3}, respectively.

Bulk measurements of b_p demonstrated more modest differences between the bay and ELS; the average for the bay (0.32 m^{-1}) was only 16% higher (Fig. 5B). However, bulk measurements of b_{bp} (Fig. 5C) were on average (0.004 m^{-1}) substantially higher in the bay than at the ELS sites, to an extent (two-fold) that approached the differences calculated for $b_{b,m}$. Differences in PAV$_m$ explained 76% of the observed variability in b_{bp} according to linear least-squares regression ($p < 0.01$); however, these were not a significant predictor of b_p dynamics.

Performance of the two-component model—Summations of minerogenic and organic scattering contributions are compared to the bulk measurements (Fig. 5B,C). These summations were close to the measurements of b_p; the average deviation was 8.2%. All but one (ELS2) of the summations of the independent model estimates were within 13% of the observations (excluding ELS2, average percentage error of ~6%). Though the linear relationship between measured values of b_p and the summations was heavily weighted by the KW1 site, an approach towards equivalency (slope 0.8) was still indicated for the other sites (Fig. 6A, and inset).

The higher PAV$_m$ and organic scattering (Fig. 5A) contributed nearly equally to the elevated b_p measured at KW1 (Fig. 5B). Levels of b_p in KB sites and ELS sites were not significantly different from each other. However, there were noteworthy spatial differences in the relative contributions of b_o and b_m to b_p (Fig. 5B). For the three pelagic ELS sites, b_o accounted for an average of 95% of b_p. In contrast, its contribution decreased to a mean of 63% (CV = 16%) for the other sites. Conversely, b_m was of minor importance to b_p at the ELS sites (~17% on average), but contributed more substantially (~34% on average) at the KW and KB sites, particularly at KB1 and KB3 (~45%). These results support the use of the empirical relationship (Eq. 3) for b_p in this waterbody.

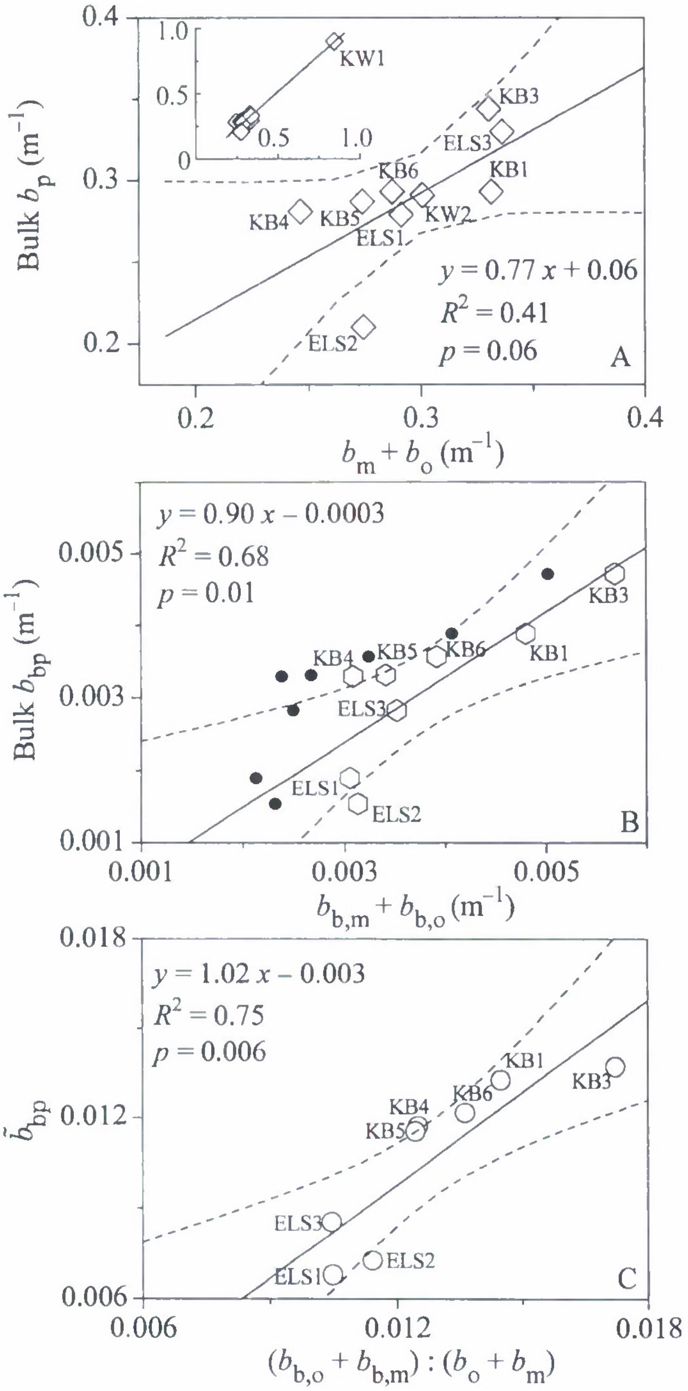

Fig. 6. Comparisons of modeling results (open symbols) with scattering measurements, with linear regression analyses (solid line: linear fit, dashed line: 95% confidence limit): (A) b_p (excluding KW1 point), with inset for all data points ($y = 1.10x - 0.04$, $R^2 = 0.98$, $p < 0.001$), (B) b_{bp}, and (C) backscattering ratio. Filled symbols in (B) represents summation result with $b_{b,o}$ predicted by an alternative model (Huot et al. 2008), and the corresponding linear regression (lines not shown) is $y = 0.87x + 0.0005$ ($R^2 = 0.72$, $p < 0.01$).

On average, the two-component model estimates of b_{bp} ($b_{b,o} + b_{b,m}$) exceeded bulk measurements by 14% (Fig. 5C). The overestimation was more pronounced for ELS sites than for the five KB sites, by an average of 63% vs. 10%. This overestimation was mainly caused by two outliers in ELS1 and ELS2, for which the [Chl]-based estimates of $b_{b,o}$ alone were greater than measured b_{bp} by 18% and 30% (Fig. 5C), respectively. Nonetheless, the two-component model performed reasonably well in representing the bulk measurements of b_{bp} (Fig. 6B). The predictions explained 68% ($p = 0.01$) of the variability in the observations, according to linear least-squares regression, with general tendency toward equivalency (slope value of 0.9) and 95% confidence limits nearly encompassing all of the data.

The relative importance of the minerogenic component was shifted higher for b_{bp} than for b_p; on average, $b_{b,m}$ accounted for 42% of the bulk measurements in the ELS sites vs. 64% overall for KB sites (exceeded 75% of the b_{bp} values for the KB1 and KB3 locations). The highest predicted b_{bp} value (0.012 m^{-1}) was for KW1, with a minerogenic contribution of 67.4% (Fig. 5C).

Backscattering ratio and its dependencies.—The backscattering ratio, $\tilde{b}_{bp}$, based on in situ measurements, was substantially lower at the ELS sites (mean = 0.0075) than the KB sites (mean = 0.0125; Fig. 5D). The estimated ratios, based on SAX results and bio-optical models [$(b_{b,o} + b_{b,m}) : (b_o + b_m)$], on average were 12% (range = 7–26%) higher than those based on bulk measurements at KB sites. However, deviations were more pronounced for the ELS sites (45% on average; Fig. 5D), associated with relatively large predicted contributions by $b_{b,o}$. The estimated ratio for KW1 was higher than that for KW2. The respective backscattering ratios of the organic and minerogenic components ($\tilde{b}_{b,o}$ and $\tilde{b}_{b,m}$) are presented in Fig. 5E for reference. Values of $\tilde{b}_{b,m}$ were uniform (mean = 0.022, CV = 7.7%) and on average more than two times higher than those of $\tilde{b}_{b,o}$ (mean = 0.009, CV = 4.7%; Fig. 5E), established by the adopted bio-optical models. The modeled $\tilde{b}_{bp}$ approached equivalency (slope value of 1.02, $R^2 = 0.75$, $p < 0.01$, intercept not significantly different from 0) with values based on bulk measurements (Fig. 6C).

The dependence of $\tilde{b}_{bp}$ values on indicators of bulk particle composition, [Chl] and the [Chl] : c_p ratio (c_p is the particulate attenuation coefficient at $\lambda = 650$ nm; Boss et al. 2004; Loisel et al. 2007), was evaluated. The ratio $\tilde{b}_{bp}$ was negatively correlated ($R = 0.81$) with log([Chl]) (Fig. 7A). Strong negative relationships also existed between $\tilde{b}_{bp}$ and [Chl] : c_p based on both measurements (Fig. 7B; $R^2 = 0.88$) and modeling (Fig. 7C; $R^2 = 0.66$). The dependence of $\tilde{b}_{bp}$ (from bulk measurements) on the ratio of $b_m : c_p$, was observed to be a strong positive relationship ($R^2 = 0.67$; Fig. 7D).

Discussion

Minerogenic particles in Lake Superior—Levels of b_p in the pelagic waters of Lake Superior and in Keweenaw Bay were low relative to most of the lacustrine systems included in the listing of Kirk (1994). The observed levels of PAV$_m$ were comparable to those reported for Skaneateles Lake (one of the Finger Lakes of New York), the system with the highest clarity among those characterized previously by SAX (Peng et al. 2007). Minerogenic particles, mostly clay

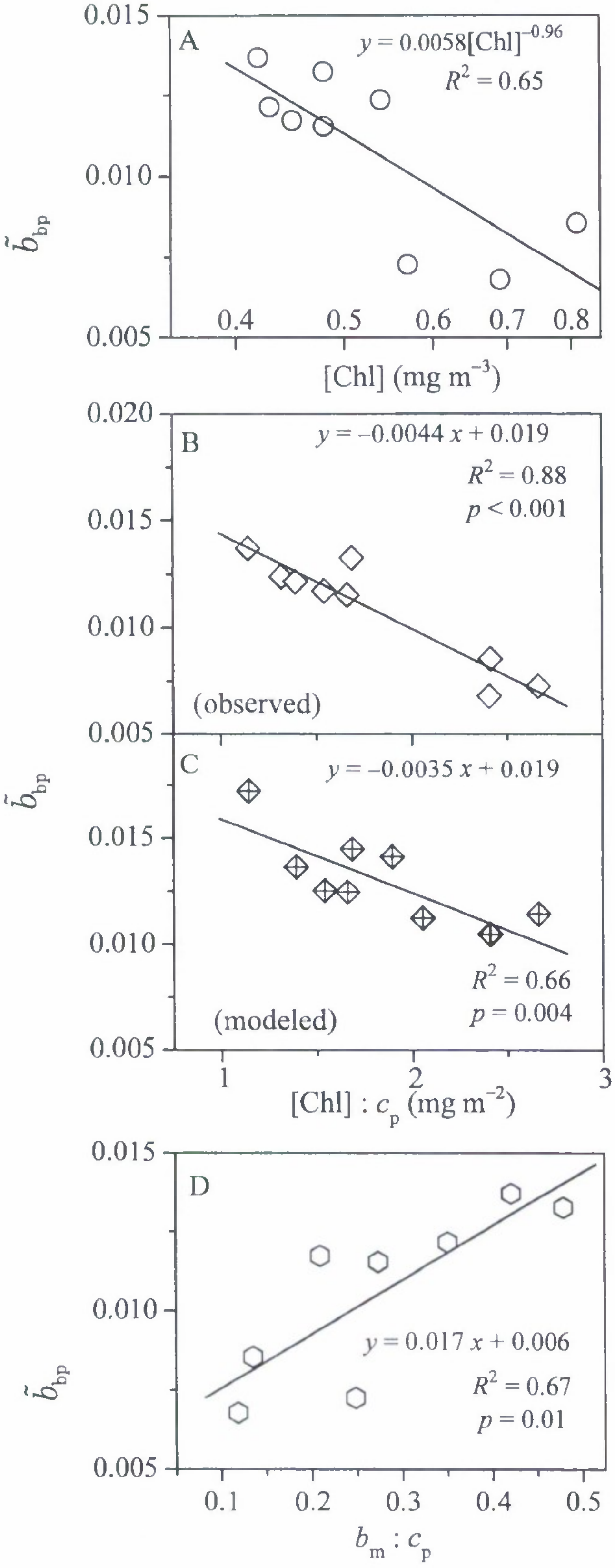

Fig. 7. Evaluations of backscattering ratio dependence (at 650 nm): (A) observed $\tilde{b}_{bp}$ as a function of [Chl] and power-law fit with χ^2 reduced to 2.7×10^{-6}, (B and C) $\tilde{b}_{bp}$ (observed and modeled) as a function of the [Chl] : c_p ratio, and (D) observed $\tilde{b}_{bp}$ as a function of the $b_m : c_p$ ratio. Linear least-squares regression results are shown in (B), (C), and (D).

minerals in the size range 1–10 μm, were an important component of backscattering in Lake Superior and Keweenaw Bay during the study, and were a significant contributor to b_p in the bay. The higher levels of PAV$_m$ in KB compared to the open waters of the ELS sites (Fig. 5A–C) presumably reflected local inputs of mineral particles from the tributary (Sturgeon River) and perhaps resuspension. Both levels and spatial heterogeneity of this scattering component were probably conservatively represented by the summertime sampling of this study. For example, >70% of the annual sediment loading to the Keweenaw area is received in spring (Auer and Gatzke 2004). Substantial sediment plumes have been described for the lake, in spring from tributary inputs (Budd 2004; Stortz et al. 1976). The documented differences in PAV$_m$ within the bay and ELS sites supports the position that such spatial structure in minerogenic particle concentrations is common. The elevated levels of b_{bp} and $b_{b,m}$ in Keweenaw Bay represent an appropriate target for resolution through remote-sensing techniques.

The high levels of $b_{b,m}$ and c_p (Loisel and Morel 1998) relative to the prevailing levels of [Chl] and their generally noncovarying character, as well as the high CDOM levels (Gons et al. 2008), make the lake and its embayments a Case 2 system. Thus, it is not surprising that application of bio-optical remote-sensing algorithms, developed for Case 1 waters, resulted in overestimations of [Chl] (Li et al. 2004). Woźniak and Stramski (2004) predicted such overestimates from the effects of minerogenic particles through Mie scattering calculations for different PSDs and refractive indices (m). Moreover, these investigators reported that PSD and m must be taken into account, rather than just the common bulk gravimetric measure of the minerogenic particle population, to quantify these effects. SAX results may be valuable in developing a more robust mechanistic algorithm for Lake Superior and other Case 2 systems.

Early comparisons to other systems—Although the number of freshwater systems studied by SAX remains modest, the general shape of the PSDs (Fig. 3) has been a recurring feature (Peng and Effler 2007; Peng et al. 2007). The observed PSD pattern is consistent with results from model simulations of particle aggregation and sedimentation in a closed system and with the conclusion that particles (individuals or aggregates) in the size range 0.1–10 μm are the most stable particulate material in aquatic systems (Buffle and Leppard 1995; Atteia 1998). The dominant role of particles in the size range 1–10 μm in regulating b_m and $b_{b,m}$ in Lake Superior and Keweenaw Bay (Fig. 4) is also documented in earlier studies. Observed differences in the relative importance of various particle sizes within this range, as represented by d_{50} values, reflect differences in the details of the various PSDs in these studies. The average d_{50} for b_m for this large lake (2.4 μm) was about one-half of those reported for much smaller lakes and a river by Peng et al. (2007). A d_{50} value of ~1 μm was reported for typical marine mineral particles (Babin et al. 2003) based on Mie theory calculations (specifications of n = 1.18, Junge function slope range =

3.8–4.2). The differences among these systems are superficially consistent with differences in sorting (e.g., settling propensity) expected for these environments (e.g., from large rivers and small lakes to large lakes, to the oceans). Both PSD and particle composition, features that may vary greatly among systems, affect the size dependency patterns of b_{p} and b_{bp}. The differences in the cumulative percent contribution per size class to b_{m} and $b_{\mathrm{b,m}}$ reported here (Fig. 4; *see also* d_{50} values in Table 1) are manifestations of the high refractive indices and PSDs of the minerogenic particle population of Lake Superior.

Clay minerals have been a prominent component of minerogenic scattering in all the characterized inland waters. The plate-like morphology of clay minerals (e.g., Fig. 2A) contributes to the persistence of these terrigenous particles in water columns (Lal and Lerman 1975; Davies-Colley et al. 2003). Calcite (not a noteworthy component in this system), in contrast, is formed autochthonously during summertime events in many productive hardwater lacustrine systems (Effler 1996; Davies-Colley et al. 2003) and has been linked to primary production (Hodell et al. 1998). This mineral can become dominant with respect to light scattering during these events (Peng and Effler 2005; Peng et al. 2007), and is irregularly important in three of the other Laurention Great Lakes—Lakes Ontario, Erie, and Michigan (Strong and Eadie 1978).

Uncertainties in SAX–Mie estimates of b_m *and* $b_{b,m}$—Sources of uncertainty related to the estimates of b_{m} and $b_{\mathrm{b,m}}$ have been addressed previously (Peng et al. 2007). A selective review of that material is included here. Because this represents the first effort to pursue closure for b_{bp} based on SAX–Mie estimates of $b_{\mathrm{b,m}}$, particular attention is given to the contrasting situation for uncertainties related to b_{m} vs. $b_{\mathrm{b,m}}$. Issues considered here are limitations of the SAX measurements and the applicability of Mie theory.

The morphological characterizations of individual particles by SAX are robust. The precision of SAX determinations of PAV$_{\mathrm{m}}$, based on replicate analyses, is about 10%. Only modest uncertainty in PA (±5%), and related scattering estimates, is attributable to the protocol adopted to adjust for the lying-flat effect (Peng and Effler 2007). There is only minor uncertainty in the placement of SAX-characterized minerogenic particles within the adopted chemical classes. However, these groups are not definitive for specific (particularly clay) minerals, thereby introducing uncertainty in the specification of the *m* value (more specifically, *n*). The most different of the common clay minerals in this regard is montmorillonite that has an *n* value about 0.045 units lower than most of the others (Woźniak and Stramski 2004). The composition of the 'Si-rich' and the unspecified 'Misc' groups (both with assumed *m* values) represents another minor source of uncertainty, because these groups only made modest contributions to PAV$_{\mathrm{m}}$ (Table 1). Mie theory estimates of $b_{\mathrm{m}}(650)$ have been reported (Peng et al. 2007) to be insensitive to a wide range of *n* values (broader than the possible deviation for clays) for the observed PSD patterns (Fig. 3). Increased sensitivity is predicted for Junge PSD cases. In contrast, estimates of $b_{\mathrm{b,m}}$ are sensitive to modest differences in *n* for the observed PSD pattern (Peng et al. 2007). For example, if montmorillonite was dominant instead of other clay minerals (as assumed here), the estimate of $b_{\mathrm{b,m}}$ could be biased ~20% high (*see* fig. 9 in Peng et al. 2007).

Most marine (Volten et al. 1998; Gordon and Du 2001) and freshwater (Peng et al. 2007; this study) particles are nonspherical, and thus do not meet the sphericity stipulation of Mie theory. Deviations from sphericity cause shifts in the VSF that influence light scattered in the backward direction more than the forward (Mishchenko and Travis 1994). Depending on the details of particle shapes, nonsphericity can cause either enhancement or diminishment of the magnitude of b_{bp} relative to spherical particles (Bohren and Huffman 1983; Volten et al. 1998; Gordon and Du 2001). The effects of this on b_{p} are generally less (Holland and Gagne 1970; Jonasz 1987). This, together with the greater sensitivity of $b_{\mathrm{bp}}(\lambda)$ to the value of *n* results in greater confidence in the estimates of b_{m} than those of $b_{\mathrm{b,m}}$. However, Liu et al. (2003) demonstrated that for nonspherical quartz particles, the deviation of the Mie-modeled phase function from that of measured had very little effect on the predicted b_{bp}. More complex models for nonspherical particles (Mishchenko and Travis 1994) would also have substantial uncertainty, given the variability in particle shapes encountered in our studies (Table 1; Peng and Effler 2007; Peng et al. 2007). Mie theory calculations presently represent the most viable alternative to estimate b_{m} and $b_{\mathrm{b,m}}$ based on single particle optics from individual particle information for large heterogeneous particle populations. The applicability of Mie theory can be expected to be more tenuous where greater deviations from sphericity are prevalent, conditions commonly encountered for biological particle assemblages such as pennate diatoms (Fig. 2B; *see* ASP values for diatoms in Table 1). The robust representations of particle shape available from SAX may prove to be valuable in advancing more complex light-scattering models for minerogenic particles.

Pursuit of optical closure—Two other sources of uncertainty need to be considered in evaluating the extent of closure: the adequacy of the empirical bio-optical models for b_{o} and $b_{\mathrm{b,o}}$, and the representativeness of bulk measurements of b_{p} and b_{bp} and collected samples. The models (Eqs. 3 and 4) developed for Case 1 oceanic waters, driven by [Chl], have demonstrated noteworthy variability in performance for those targeted ecosystems (Morel and Maritorena 2001). A major contributor to this variability is the imperfect character of [Chl] as a surrogate of optical properties (Morel and Maritorena 2001). The dispersion in the b_{p}–[Chl] relationships in Case 1 waters has been described as "definitely large" (p. 7177; Morel and Maritorena 2001). Substantially greater uncertainty in estimates of $b_{\mathrm{b,o}}$ compared to that of b_{o} is acknowledged. The exceedence of b_{bp} by $b_{\mathrm{b,o}}$ estimates at ELS1 and ELS2 (Fig. 5C) suggests overestimation of the organic component in these cases by the bio-optical model (Eq. 4b). Divergent b_{bp}–[Chl] relationships have been published, but without compelling validation (Morel and Maritorena 2001). Use of an alternative relationship (Huot et al. 2008) developed from paired $b_{\mathrm{bp}}(650)$ and [Chl] observations in Case 1 waters caused ~40% decreases in predictions of $b_{b,o}$, but resulted in similar performance in explaining the observed variability in bulk measurements with the two-component model (Fig. 6B).

This analysis in this study invokes a scattering component for organic particles in Lake Superior that corresponds to Case 1 conditions. The range of [Chl] in the lake is within that covered in the development of the bio-optical models. Other covarying scattering particles potentially embedded within these relationships include organic detritus and minerogenic particles. The assumptions implicit in adoption of Case 1 relationships in our two-component model are that any embedded detritus is representative for the lake, and that any embedded minerogenic component is insignificant compared with the independent SAX–Mie estimates of b_m and $b_{b,m}$ (i.e., the extent of 'double counting' of this component is negligible).

The variability in the multiple observations of b_p and b_{bp} within the depth interval of measurements was relatively minor, with average CVs of 2.6% and 5.5%, respectively. The uncertainty in the bulk measurement of b_{bp}, associated with estimation based on a single backward angle measurement (~10%; Boss and Pegau 2001), is greater than for b_p. Whitmire et al. (2007) evaluated multiple sources of uncertainty for $\tilde{b}_{bp}(\lambda)$ and presented a likely maximum error in the ratio of ~20%, a magnitude that is modest relative to the observed variability (Fig. 5D). Finally, the widely acknowledged patchy distribution of particles (Babin et al. 2003) results in the imperfect representation of bulk conditions and by water samples collected in temporal and spatial proximity.

The credibility of the SAX–Mie estimates of minerogenic scattering in Lake Superior is supported by their consistency and the extent of closure with bulk measurements through the two-component approach (Figs. 5B–D, 6). This performance for such a dilute system and the addition of closure analyses for backscattering (Figs. 5C, 6B) substantially augments earlier efforts to test the credibility of the SAX–Mie approach in other lacustrine systems (Peng and Effler 2007; Peng et al. 2007). The weight of continuing successful applications, over an increasingly diverse array of systems, provides the strongest case for the credibility and applicability of the approach. This study did not provide a rigorous test of the credibility of b_m estimates for the ELS sites because of the minor contributions of this component to b_p. However, the differences in this component between these sites and those in the embayment and at KW1 were reasonably well-supported (Figs. 5B, 6A). The greater uncertainties in $b_{b,m}$ estimates, and contributing components of related closure analyses of $b_{b,o}$ estimates and b_{bp} measurements, are compensated for by the stronger signal of minerogenic particles for b_{bp} compared to b_p. The extent of closure for b_{bp} (Fig. 6B) was actually somewhat better than that for b_p (Fig. 6A). Much, if not all, of the observed shortcomings in closure is well within the accepted variability in the empirical bio-optical models for Case 1 waters adopted here for the organic components. Moreover, the paradigms describing the dependence of $\tilde{b}_{bp}$ on the relative contributions of organic and inorganic particles to the overall particle assemblage were well-supported by the results from the SAX–Mie approach (Fig. 7C,D).

The demonstrated extent of closure has implications with respect to pathways to assess scattering conditions in Lake Superior as well as other systems. First, reasonable first approximations of the organic component can be made from widely available [Chl] data. Paired observations of PAV_m and [Chl], through this simple two-component model, can be used to estimate the bulk scattering metrics of b_p and b_{bp}, and partition these into organic and multiple minerogenic components. The availability of SAX observations is presently limited. However, these findings further suggest that reasonable first estimates of b_m and $b_{b,m}$ can be made for Case 2 waters enriched in minerogenic particles for which observations of b_p, b_{bp}, and [Chl] are available (Loisel et al. 2007; Whitmire et al. 2007), based on residual calculations ($b_{b,m} = b_{bp} - b_{b,o}$). Conversely, b_o and $b_{b,o}$ can be estimated from SAX and bulk b_p and b_{bp}.

Backscattering ratio at 650 nm—This ratio, $\tilde{b}_{bp}$, is independent of particle concentration, with which b_p and b_{bp} co-vary linearly. It depends instead on the chemical composition, PSD, and particle shape(s) of the assemblage. Thus, $\tilde{b}_{bp}$ represents a source of information for these attributes. Measurements of $\tilde{b}_{bp}$ have been used to describe the variability of the bulk refractive index (n) of oceanic particle populations (Twardowski et al. 2001; Boss et al. 2004; Sullivan et al. 2005). Low n values correspond to dominance by phytoplankton, whereas high values reflect dominance by minerogenic particles (Loisel et al. 2007; Whitmire et al. 2007). In addition to supporting inferences of particle composition, the ratio is valuable in modeling the underwater light field (Mobley et al. 2002).

The number of observations of $\tilde{b}_{bp}$ for this study is small compared with surveys reported for several marine systems (Loisel et al. 2007; Whitmire et al. 2007; Snyder et al. 2008). However, our observations are interesting in the context of the strength of the observed relationships with [Chl] (Fig. 7A) and its contribution to total particulate matter ([Chl] : c_p; Fig. 7B), and the availability of the two-component model estimates of the ratio (Fig. 7C) and direct minerogenic scattering (Fig. 7D). The two-fold difference in the ratio reported here was similar to that observed in the survey of several Central New York systems (Peng et al. 2007). The variability within the upper waters of Crater Lake was apparently less, with only 17% difference between the 10th and the 90th percentiles of the observations (Whitmire et al. 2007). Much broader ranges (e.g., >10-fold differences) in $\tilde{b}_{bp}$ were reported in larger marine surveys (Boss et al. 2004; Loisel et al. 2007; Whitmire et al. 2007). However, the central tendency of the Lake Superior observations was similar to the other studies; for example, the mean was 0.0108, compared with 0.010 reported by Whitmire et al. (2007) and 0.0138 (geometric mean) by Loisel et al. (2007).

The performance of the power-law fit ($R^2 = 0.65$, Fig. 7A) describing the dependence of $\tilde{b}_{bp}$ on [Chl] compares favorably with those reported elsewhere (Twardowski et al. 2001; Sullivan et al. 2005; Whitmire et al.

2007). However, this model is mechanistically weak, and in this case inappropriate, because it fails to accommodate the documented spatial differences in minerogenic scattering (Fig. 5C) that did not covary with [Chl] (Fig. 5A). The dependence of $\tilde{b}_{bp}(\lambda)$ on the ratio [Chl]$:c_p(\lambda)$ is more mechanistically sound, because this ratio serves as a proxy for the relative proportion of phytoplankton within the overall particle assemblage (Boss et al. 2004; Loisel et al. 2007), and it was stronger ($R^2 = 0.88$; Fig. 7B). Decreases of $\tilde{b}_{bp}$ reflect increases in the contribution of phytoplankton to the light-scattering particle assemblage (Boss et al. 2004; Loisel et al. 2007). The slope of the Lake Superior relationship (-0.0044) is similar to that (-0.0066) reported by Boss et al. (2004) between observed $\tilde{b}_{bp}(532)$ and [Chl]$:c_p(660)$. The relationship remained strong for the backscattering ratio based on the two-component model (Fig. 7C).

The greater strength of the observed $\tilde{b}_{bp}$ vs. [Chl]$:c_p$ relationship ($R^2 = 0.88$) for the single cruise compared to larger marine surveys is noteworthy. For example, the relationships reported by Boss et al. (2004) and Loisel et al. (2007) explained 56% and 26% of the observed $\tilde{b}_{bp}$ variability. This suggests greater uniformity in the monitored light-scattering features of particles in Lake Superior for this single cruise. A contributing factor is the similar light-scattering characteristics of the minerogenic particle populations other than N (Figs. 3, 4, 5E; Table 1). The strength of the observed $\tilde{b}_{bp}$ – [Chl]$:c_p$ relationship further suggests a relatively uniform cellular content of chlorophyll *a* for the narrow [Chl] range observed here. Greater variability in this relationship (Fig. 7B) may arise from year-round monitoring as the cellular content of this pigment (Reynolds 2006) shifts, even if the light-scattering attributes of the minerogenic particles remain unchanged. However, it remains that over this brief interval the ratio [Chl]$:c_p$ was a strong predictor of observed $\tilde{b}_{bp}$. The Lake Superior results suggest that the relationship may be substantially stronger within individual systems than those observed for broad cross-sectional studies (Loisel et al. 2007; Whitmire et al. 2007).

A corollary interpretation of the observed relationship between $\tilde{b}_{bp}$ and [Chl]$:c_p$ (Fig. 7B) described elsewhere has been that the contribution of minerogenic particles to the light-scattering particle assemblage increases as $\tilde{b}_{bp}$ increases (Twardowski et al. 2001; Boss et al. 2004; Loisel et al. 2007). Although this position has been supported by corresponding estimates of bulk refractive index, it has not been rigorously supported by paired direct measurements of the inorganic particle population. The estimates of b_m provide the opportunity to directly test that interpretation for this study. Indeed, a strong ($R^2 = 0.67$) positive relationship prevailed between $\tilde{b}_{bp}$ and the ratio $b_m : c_p$ for this study (Fig. 6D), directly supporting the position that $\tilde{b}_{bp}$ increases as the fraction of light scattering associated with minerogenic particles increases. A similarly strong relationship was observed when the b_m estimates in the ratio were replaced by the PAV$_m$ measurements. The calculated $\tilde{b}_{bp}$ values for hypothetical cases of strictly minerogenic or phytoplankton populations (Fig. 5E) can be considered as bounding conditions for this system. The observed intermediate values (Fig. 5D) represented the outcomes of mixtures with varying contributions from the minerogenic and organic (phytoplankton) particle populations.

Implications—The integrated SAX–Mie approach offers great promise for enhancing the understanding of the role of minerogenic particles in influencing the underwater light field and remote-sensing signals. Applications of this approach advance implementation of the reductionist strategy for better understanding of the real complex optical regimes through quantitative partitioning of the effects of organic vs. multiple minerogenic constituents. Inclusion of SAX characterizations in the suite of measurements of optics monitoring programs would provide independent measurements of PSD and composition for multiple constituents within minerogenic particle populations, thereby avoiding the need for arbitrary specifications in related modeling efforts. This represents an invaluable reduction in the 'degrees of freedom' of the modeling process by providing independent key inputs, widely sought by the modeling community to improve the credibility of such frameworks (Chapra 1997). SAX information has potential value for a wide range of issues, such as to address origins of backscattering in oceanic waters (Stramski et al. 2004*a*), and to aid in establishing management targets and reasonable expectations for programs intended to increase clarity in inland waters (Effler et al. 2008).

This study of Lake Superior has enhanced the case for the credibility of the SAX–Mie approach to independently quantify b_m, and has provided a valuable and encouraging first test of the capability for $b_{b,m}$. Lake Superior has represented a challenging test for inland water application because of the relatively dilute nature of this system, thereby providing optimism for successful application for more spatially and temporally robust descriptions of this lake and for other dilute systems, including the other Laurentian Great Lakes and oceanic waters. Moreover, increased support for $\tilde{b}_{bp}$ as a surrogate metric of the contribution of minerogenic particles to overall scattering has been provided.

Much broader applications of the SAX–Mie approach, in concert with the bulk measurements of b_p and b_{bp} included here, are recommended to (1) further test the consistency and related extent of closure for these forward estimates of light scattering, (2) demonstrate the utility of the increased partitioning capability of the minerogenic component, and (3) advance the testing of $\tilde{b}_{bp}$ as a metric of the relative contributions of minerogenic particles to overall scattering. Increased testing is particularly necessary for SAX–Mie-based estimates of $b_{b,m}$ to enhance the case for the credibility of these estimates and to represent associated effects on the remote-sensing signal.

Acknowledgments

Funding for this research was provided in part by Naval Research Laboratory for the 'Lidar and hyperspectral remote sensing of the littoral environment' project. Sampling and field optical measurements were assisted by Tony Prestigiacomo aboard the U.S. Environment Protection Agency's R/V *Lake Guardian* (pelagic waters of Lake Superior) and Michigan Technological University's R/V *Agassiz* (Keweenaw Bay). Laboratory analyses of chlorophyll *a* concentrations were performed by Whitney Forbes. U.S. Environmental Protection Agency graciously contributed ship time aboard the R/V *Lake Guardian* to Michigan Tech as part of a cruise combining graduate instruction and value-added research. We thank the Associate Editor, Dariusz Stramski, and two other anonymous reviewers for their instructive comments. This is contribution 263 of the Upstate Freshwater Institute.

References

Atteia, O. 1998. Evolution of size distributions of natural particles during aggregation: Modelling versus field results. Colloid. Surface. A **139:** 171–188, doi:10.1016/S0927-7757(98)00279-9.

———, D. Perret, T. Adatte, R. Kozel, and P. Rossi. 1998. Characterization of natural colloids from a river and spring in a karstic basin. Environ. Geol. **34:** 257–269, doi:10.1007/s002540050277.

Auer, M. T., and T. L. Gatzke. 2004. The spring runoff event, thermal bar formation, and cross margin transport in Lake Superior. J. Great Lakes Res. (suppl. 1) **30:** 64–81.

Babin, M., A. Morel, V. Fournier-Sicre, F. Fell, and D. Stramski. 2003. Light scattering properties of marine particles in coastal and open ocean waters as related to the particle mass concentration. Limnol. Oceanogr. **48:** 843–859.

Bohren, C. F., and D. R. Huffman. 1983. Absorption and scattering of light by small particles. Wiley.

Boss, E., and W. S. Pegau. 2001. Relationship of light scattering at an angle in the backward direction to the backscattering coefficient. Appl. Opt. **40:** 5503–5507.

———, ———, M. Lee, M. Twardowski, E. Shybanov, G. Korotaev, and F. Baratange. 2004. Particulate backscattering ratio at LEO 15 and its use to study particle composition and distribution. J. Geophys. Res. **109:** C01014, doi:10.1029/2002JC001514.

Budd, J. W. 2004. Large-scale transport phenomena in the Keweenaw region of Lake Superior: The Ontonagon plume and the Keweenaw eddy. J. Great Lakes Res. (suppl. 1) **30:** 467–480.

Buffle, J., and G. G. Leppard. 1995. Characterization of aquatic colloids and macromolecules. 1. Structure and behavior of colloidal material. Environ. Sci. Technol. **29:** 2169–2175, doi:10.1021/es00009a004.

Bukata, R. P., J. H. Jerome, J. E. Bruton, and E. B. Bennett. 1978. Relationship among optical transmission, volume reflectance, suspended mineral concentration, and chlorophyll *a* concentration in Lake Superior. J. Great Lakes Res. **4:** 456–461.

Chapra, S. C. 1997. Surface water-quality modeling. McGraw-Hill.

Davies-Colley, R. J., W. N. Vant, and D. G. Smith. 2003. Colour and clarity of natural waters: Science and management of optical water quality. Blackburn Press.

Effler, S. W. 1996. Limnological and engineering analysis of a polluted urban lake: Prelude to environmental management of Onondaga Lake, New York. Springer.

———, R. K. Gelda, M. G. Perkins, F. Peng, N. G. Hairston Jr., and C. M. Kearns. 2008. Patterns and modeling of the long-term optics record of Onondaga Lake, New York. Fundam. Appl. Limnol. **172:** 217–237, doi:10.1127/1863-9135/2008/0172-0217.

Gons, H. J., M. T. Auer, and S. W. Effler. 2008. MERIS satellite chlorophyll mapping of oligotrophic and eutrophic waters in the Laurentian Great Lakes. Remote Sens. Environ. **112:** 4098–4106, doi:10.1016/j.rse.2007.06.029.

Gordon, H. R., and T. Du. 2001. Light scattering by nonspherical particles: Application to coccoliths detached from *Emiliania huxleyi*. Limnol. Oceanogr. **46:** 1438–1454.

Green, R. E., H. M. Sosik, and R. J. Olson. 2003. Contributions of phytoplankton and other particles to inherent optical properties in New England continental shelf waters. Limnol. Oceanogr. **48:** 2377–2391.

Hodell, D. A., C. L. Schelske, G. L. Fahnenstiel, and L. L. Robbins. 1998. Biologically induced calcite and its isotopic composition in Lake Ontario. Limnol. Oceanogr. **43:** 187–199.

Holland, A. C., and G. Gagne. 1970. The scattering of polarized light by polydisperse systems of irregular particles. Appl. Opt. **9:** 1113–1121.

Huot, Y., A. Morel, M. S. Twardowski, D. Stramski, and R. A. Reynolds. 2008. Particle optical backscattering along a chlorophyll gradient in the upper layer of the eastern South Pacific Ocean. Biogeosciences **5:** 495–507.

Jonasz, M. 1987. Nonsphericity of suspended marine particles and its influence on light scattering. Limnol. Oceanogr. **32:** 1059–1065.

Kerr, P. F., and A. F. Rogers. 1977. Optical mineralogy, 4th ed. McGraw-Hill.

Kirk, J. T. O. 1994. Light and photosynthesis in aquatic ecosystems, 2nd ed. Cambridge Univ. Press.

Lal, D., and A. Lerman. 1975. Size spectra of biogenic particles in ocean water and sediments. J. Geophys. Res. **80:** 423–430.

Li, H., J. W. Budd, and S. Green. 2004. Evaluation and regional optimization of bio-optical algorithms for Central Lake Superior. J. Great Lakes Res. (suppl. 1) **30:** 443–458.

Liu, L., M. I. Mishchenko, J. W. Hovenier, H. Volten, and O. Muñoz. 2003. Scattering matrix of quartz aerosols: Comparison and synthesis of laboratory and Lorenz-Mie results. J. Quant. Spectrosc. Radiat. Transfer **79:** 911–920, doi:10.1016/S0022-4073(02)00328-X.

Loisel, H., X. Mériaux, J.-F. Berthon, and A. Poteau. 2007. Investigation of the optical backscattering to scattering ratio of marine particles in relation to their biogeochemical composition in the eastern English Channel and southern North Sea. Limnol. Oceanogr. **52:** 739–752.

———, and A. Morel. 1998. Light scattering and chlorophyll concentration in case 1 waters: A reexamination. Limnol. Oceanogr. **43:** 847–858.

Lubac, B., and H. Loisel. 2007. Variability and classification of remote sensing reflectance spectra in the eastern English Channel and southern North Sea. Remote Sens. Environ. **110:** 45–58, doi:10.1016/j.rse.2007.02.012.

Mishchenko, M. I., and L. D. Travis. 1994. Light scattering by polydispersions of randomly oriented spheroids with sizes comparable to wavelengths of observation. Appl. Opt. **33:** 7206–7225.

Mobley, C. D., L. K. Sundman, and E. Boss. 2002. Phase function effects on oceanic light fields. Appl. Opt. **41:** 1035–1050.

Morel, A., and S. Maritorena. 2001. Bio-optical properties of oceanic waters: A reappraisal. J. Geophys. Res. **106:** 7163–7180, doi:10.1029/2000JC000319.

Parsons, T. R., Y. Maita, and C. M. Lalli. 1984. A manual of chemical and biological methods for seawater analysis, 1st ed. Pergamon Press.

Pegau, W. S., D. Gray, and J. R. V. Zaneveld. 1997. Absorption and attenuation of visible and near-infrared light in water: Dependence on temperature and salinity. Appl. Opt. **36:** 6035–6046.

Peng, F., and S. W. Effler. 2005. Inorganic tripton in the Finger Lakes of New York: Importance to optical characteristics. Hydrobiologia **543:** 259–277, doi:10.1007/s10750-004-7892-2.

———, and ———. 2007. Suspended minerogenic particles in a reservoir: Light-scattering features from individual particle analysis. Limnol. Oceanogr. **52:** 204–216.

———, ———, D. M. O'Donnell, M. G. Perkins, and A. D. Weidemann. 2007. Role of minerogenic particles in light scattering in lakes and a river in central New York. Appl. Opt. **46:** 6577–6594.

———, D. L. Johnson, and S. W. Effler. 2002. Suspensoids in New York City's drinking water reservoirs: Turbidity apportionment. J. Am. Water Resour. Assoc. **38:** 1453–1465.

Reynolds, C. S. 2006. Ecology of phytoplankton. Cambridge Univ. Press.

Snyder, W. A., and others. 2008. Optical scattering and backscattering by organic and inorganic particulates in U.S. coastal waters. Appl. Opt. **47:** 666–677.

Stavn, R. H., and S. J. Richter. 2008. Biogeo-optics: Particle optical properties and the partitioning of the spectral scattering coefficient of ocean waters. Appl. Opt. **47:** 2660–2679.

Stortz, K., R. Clapper, and M. Sydor. 1976. Turbidity sources in Lake Superior. J. Great Lakes Res. **2:** 393–401.

Stramski, D., M. Babin, and S. B. Woźniak. 2007. Variations in the optical properties of terrigenous mineral-rich particulate matter suspended in seawater. Limnol. Oceanogr. **52:** 2418–2433.

———, E. Boss, D. Bogucki, and K. J. Voss. 2004*a*. The role of seawater constituents in light backscattering in the ocean. Progr. Oceanogr. **61:** 27–56.

———, A. Bricaud, and A. Morel. 2001. Modeling the inherent optical properties of the ocean based on the detailed composition of the planktonic community. Appl. Opt. **40:** 2929–2945.

———, and D. A. Kiefer. 1991. Light scattering by microorganisms in the open ocean. Progr. Oceanogr. **28:** 343–383.

———, S. B. Woźniak, and P. J. Flatau. 2004*b*. Optical properties of Asian mineral dust suspended in seawater. Limnol. Oceanogr. **49:** 749–755.

Strong, A. E., and B. J. Eadie. 1978. Satellite observations of calcium carbonate precipitations in the Great Lakes. Limnol. Oceanogr. **23:** 877–887.

Sullivan, J. M., M. S. Twardowski, P. L. Donaghay, and S. A. Freeman. 2005. Use of optical scattering to discriminate particle types in coastal waters. Appl. Opt. **44:** 1667–1680.

Swift, T. J., J. Perez-Losada, S. G. Schladow, J. E. Reuter, A. D. Jassby, and C. R. Goldman. 2006. Water clarity modeling in Lake Tahoe: Linking suspended matter characteristics to Secchi depth. Aquat. Sci. **68:** 1–15, doi:10.1007/s00027-005-0798-x.

Sydor, M., and R. A. Arnone. 1997. Effect of suspended particulate and dissolved organic matter on remote sensing of coastal and riverine waters. Appl. Opt. **36:** 6905–6912.

Twardowski, M. S., E. Boss, J. B. Macdonald, W. S. Pegau, A. H. Barnard, and J. R. V. Zaneveld. 2001. A model for estimating bulk refractive index from the optical backscattering ratio and the implications for understanding particle composition in case I and case II waters. J. Geophys. Res. **106:** 14,129–14,142.

Volten, H., and others. 1998. Laboratory measurements of angular distributions of light scattered by phytoplankton and silt. Limnol. Oceanogr. **43:** 1180–1197.

WET Labs, Inc. 2006. Spectral absorption and attenuation meter ac-s: User's guide. Philomath (OR): WET Labs, Inc. [accessed 2009 April 23]. Available from http://www.wetlabs.com/products/pub/acs/acsj.pdf

———. 2007. Scattering meter BB9: User's guide. Philomath (OR): WET Labs, Inc, [accessed 2009 April 23]. Available from http://www.wetlabs.com/products/pub/eco/bb9j.pdf

Whitmire, A. L., E. Boss, T. J. Cowles, and W. S. Pegau. 2007. Spectral variability of the particulate backscattering ratio. Opt. Express **15:** 7019–7031.

Woźniak, S. B., and D. Stramski. 2004. Modeling the optical properties of mineral particles suspended in seawater and their influence on ocean reflectance and chlorophyll estimation from remote sensing algorithms. Appl. Opt. **43:** 3489–3503.

Associate editor: Dariusz Stramski

Received: 07 October 2008
Accepted: 06 March 2009
Amended: 30 March 2009